Journal of Nuclear Materials 174 (1990) 168–177
North-Holland

Nucleation and growth theory of cavity evolution under conditions of cascade damage and high helium generation

N.M. Ghoniem

Mechanical, Aerospace and Nuclear Engineering Department, School of Engineering and Applied Science, University of California – Los Angeles, Los Angeles, CA 90024, USA

The evolution of helium-filled cavities during neutron irradiation is analyzed in terms of the stochastic theory of atomic clustering. The conventional separation of nucleation and growth is replaced by a self-consistent evolution model. Starting from kinetic rate (master) equations for the clustering of helium and vacancies, helium mobility, helium–vacancy cluster stability, and cavity nucleation and growth are all included in the model. Under typical fusion irradiation conditions (cascade damage and high helium-to-dpa ratios), the following is suggested: (1) Helium mobility decreases with the evolution of the microstructure. At quasi-steady state, it is mainly controlled by interstitial replacement or thermal desorption. (2) Gas re-solution from cavities by cascades increases nucleation at high fluences. (3) The cavity size distribution is broadened because of cascade-induced fluctuations. (4) The majority of helium-filled cavities are in a nonequilibrium thermodynamic state.

1. Introduction

Under the neutron irradiation conditions expected in fusion reactor structural materials, the evolution of microstructures cannot be easily described by the conventional separation into sequential nucleation and growth phases. In particular, helium-filled cavity formation proceeds via competitive reaction mechanisms which render the conventional viewpoint inapplicable. For example, the mobility of helium atoms is dictated by the evolving cavity microstructure. Since helium mobility is controlled by the rates of trapping and detrapping from various helium–vacancy (HV) clusters, it would be inappropriate to assume that it is a constant value. Because cavity nucleation is determined by helium mobility, the two processes are therefore interdependent. Collision cascades interact directly with helium atoms inside cavities and can result in their displacement back into the matrix. This process, called gas re-solution, is dynamic and continuous, resulting in re-nucleation of smaller size cavities, provided that a significant amount of helium has already been introduced into the solid. Nucleation is therefore not terminated, as assumed in classical nucleation theories, but continuously supplies freshly formed small cavities. Nucleation and growth of cavities are strongly coupled under these circumstances, and the "mean field" approximation used in the rate theory of cavity growth is poor.

Classical nucleation theory was originally applied to the nucleation of voids with no gas assistance. When the theory is used to predict the conditions for condensation of water vapor in air, liquid droplets are found to form at a critical value of the supersaturation ratio (about 5 to 6). As soon as the liquid droplets form, the supersaturation ratio abruptly drops and thereby terminates nucleation. The success of classical nucleation theory critically depends on this aspect. However, these conditions are not met under irradiation because of the continuous production of point defects and gas atoms. The theory (developed independently by Katz and Wiedersich [1] and Russell [2]), and its extensions, display several unsettling characteristics. First, nucleation rates and not cavity densities can be predicted. Second, computed nucleation rates are extremely sensitive to the physical parameters (e.g., the interstitial/vacancy arrival

0022-3115/90/$03.50

ratio, surface energy, and gas pressure). When gas production is predominant, however, as in nuclear fuels or in fusion structural materials, terminal cavity densities can be obtained. The work of Greenwood [3] and of Trinkaus [4,5] are examples of this approach.

Growth of gas-filled cavities has been treated within the framework of the mean field approximation where statistical variations in time and space are averaged. The original developments of Brailsford and Bullough [6], Bullough et al. [7], and many others (e.g., refs. [8–11]) have been successful in explaining the gross features of many experimental observations on cavity growth. However, under fusion conditions, the high helium-generation rates and the presence of collision cascades require consideration of additional physical mechanisms which influence the details of cavity growth.

In this paper we give a concise description of our work on HV-cluster evolution under irradiation, as applied to fusion reactor conditions. Analysis of helium transport and its coupling with the transient nucleation of small HV clusters is provided in section 2. A stochastic approach to the coupled nucleation/growth problem is given in section 3. The effects of single- and multiple-atom absorption and loss from an HV cluster are incorporated into the framework of Fokker–Planck theory given in section 4. The resulting equation which describes the evolution of the size distribution is solved by a two-moment approximation in section 5. Results for the effects of high helium-generation rates and collision cascades are discussed in section 6, and conclusions are given in section 7.

2. Transient helium transport and nucleation

Helium migration and transport is a time-dependent process controlled by the density and distribution of helium traps and by the trapping/detrapping rate of each. Since most helium traps are in the form of single vacancies or small vacancy clusters, it is obvious that helium transport is intrinsically coupled with the nucleation of small HV clusters. As an interstitial atom, helium mobility is very high. Unless helium is migrating between traps, it will be transported quickly to grain boundaries causing severe embrittlement. Therefore, any mechanism that enhances the speed of matrix trapping will be advantageous in preventing grain boundary absorption of helium. To determine the transport and nucleation rates of helium, a model was developed for the reactions between the three primary species (i.e., vacancies, interstitials, and helium) [12].

Rate equations are developed for the concentrations of the following species: (1) free vacancies, C_v; (2) self-interstitial atoms, C_i; (3) interstitial helium atoms, C_g; (4) substitutional helium atoms, C_{gv}; (5) di-interstitial helium atom clusters, C_{2g}; (6) di-helium, single vacancy clusters, C_{2gv}; (7) and bubble nuclei containing three helium atoms, C^*. These are given by:

$$dC_v/dt = fG + (\beta e_1 + \delta)C_{gv} - \left[\alpha C_i + \beta C_g + \gamma\left(C_s^v + C_{gv} + 2C_{2g} + 2C_{2gv} + 3C^*\right)\right]C_v, \tag{1}$$

$$dC_i/dt = fG - \left(C_v + C_{gv} + 2C_{2gv} + 3C^* - C_s^i\right)\alpha C_i, \tag{2}$$

$$\begin{aligned} dC_g/dt = {} & G_H + (\beta e_1 + \delta + \alpha C_i)C_{gv} + (\beta e_2 + 2\delta)C_{2gv} + 3(\delta + \alpha C_i)C^* \\ & + 4\delta C_{2g} + 4\alpha C_i C_{2gv} + m\delta_{tot} + \delta M_{gb} + \delta M_{ppt} - \left[\epsilon C_{tot} + C_v + 4C_g + C_{gv}\right. \\ & \left. + 2C_{2g} + 2C_{2gv} + C_{gb} + \epsilon_{ppt}C_{ppt}\right]\beta C_g, \end{aligned} \tag{3}$$

$$dC_{gv}/dt = \beta C_g C_v + (e_2 + 2\delta)C_{2gv} - (e_1 + \beta C_g + \delta + \delta C_v + \alpha C_i)C_{gv}, \tag{4}$$

$$dC_{2g}/dt = 2\beta C_g^2 + 3\alpha C_i C^* - (2\gamma C_v + 2\beta C_g + 2\delta)C_{2g}, \tag{5}$$

$$dC_{2gv}/dt = \beta C_g C_{gv} + 3\delta C^* + 2\gamma C_v C_{2g} - (2\beta C_g + 2\delta + \beta e_2 + 2\delta C_v + 2\alpha C_i)C_{2gv}, \tag{6}$$

$$dC^*/dt = 2(C_{2g} + C_{2gv})\beta C_g - 3(\beta C_g + \gamma C_v + \alpha C_i + \delta)C^*, \tag{7}$$

$$dM_{ppt}/dt = \epsilon_{ppt}\beta C_{ppt} C_g - \delta M_{ppt}, \tag{8}$$

$$dM_{gb}/dt = \beta C_{gb} C_g - \delta M_{gb}. \tag{9}$$

The definitions of various reaction rates are given in the Nomenclature. Four basic reaction frequencies are used in our analysis:

$\alpha = 48\nu_i \exp(-E_i^m/kT)$ (s^{-1}) (self-interstitial reaction frequency),
$\beta = 48\nu_g \exp(-E_g^m/kT)$ (s^{-1}) (helium reaction frequency),
$\gamma = 48\nu_v \exp(-E_v^m/kT)$ (s^{-1}) (vacancy reaction frequency),
$\delta = bG$ (s^{-1}), (radiation resolution frequency),

where the atomic jump frequencies are denoted by $\nu_{i,g,v}$ and the migration frequencies by $E^m_{i,g,v}$. The re-solution parameter, b, is defined as the probability per displacement for dissolving a helium atom back into the matrix. The emission probabilities, e_1 through e_5, are computed from binding energies, as outlined in ref. [12].

Numerical solutions to the reaction rate equations have been developed, and the concentrations were computed as functions of irradiation time. Two major quantities can be obtained from this analysis: (1) the "effective" helium diffusion coefficient and (2) the time-dependent cavity nucleation current. We will show results for the helium diffusion coefficient in this section and will then proceed to describe nucleation and growth of HV clusters.

Helium transport in an irradiated material occurs by one of several mechanisms or channels. A convenient way of defining the effective diffusion coefficient, D^e_{He}, is to take the weighted mean of all channels:

$$D^e_{He} = \sum_i D^i_{He} C^i_{He} / \sum_i C^i_{He}, \tag{10}$$

where D^i_{He} and C^i_{He} are, respectively, the diffusion coefficient of helium and its concentration in channel i. Obviously, the dominant channel will be the one with the highest helium concentration and the highest mobility. This turned out to be a complicated situation during transients, since clustering must be taken into account. Under typical reactor conditions, the length of the transient is strongly dependent upon the temperature and initial sink structure (see refs. [12] and [13]). During steady state, however, the effective diffusion coefficient can be obtained by simple analysis (see refs. [4,13,14]). Fig. 1 shows the effective helium migration energy as a function of temperature for nickel at a displacement damage rate of 10^{-6} dpa/s. The results are shown after an initial transient (i.e., at quasi-steady state), and are shown for both numerical calculations of the equations and approximate analytical solutions. The mobility of helium is determined (a) at low temperatures by radiation displacement from atomic-size traps, (b) at intermediate temperatures by the interstitial replacement mechanism, and (c) at higher temperatures by the thermal detrapping mechanism. The abrupt jumps in the migration energy are the result of analytical approximations. They indicate the approximate temperature boundaries for the various dominant mechanisms in nickel under reactor irradiation conditions. Helium mobility by the vacancy mechanism has also been considered by Trinkaus [4] and by Forman and Singh [14].

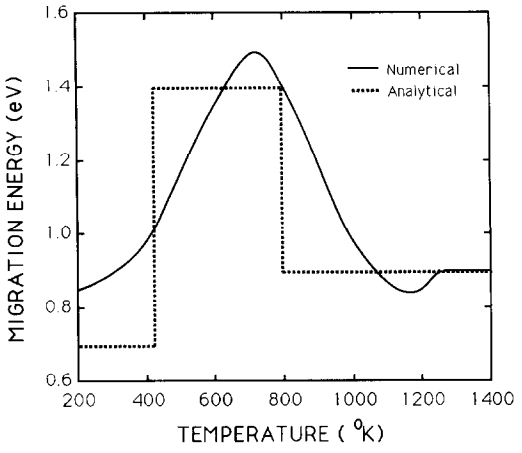

Fig. 1. Effective helium migration energy for Ni under reactor irradiation as a function of temperature.

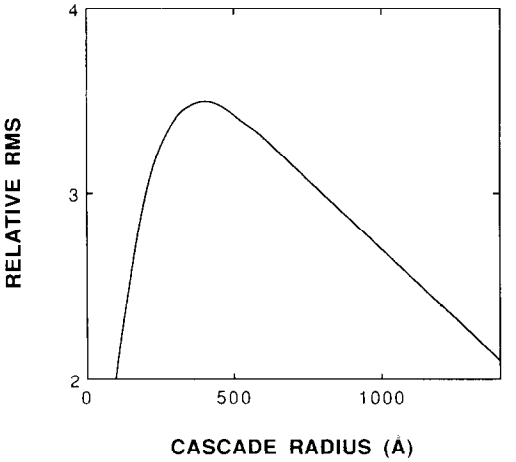

Fig. 2. Dependence of the relative root-mean-square (RMS) for vacancy concentration of the fluctuation amplitude on cascade size.

3. Stochastic description of nucleation/growth

Following Russell [15], we represent an HV cluster as a point in a two-dimensional (2D) HV phase space. The dynamical equations of motion of this point (h, v) can be written as a set of two Langevin-type equations for the velocity components as:

$$\dot{h} = \mathrm{d}h/\mathrm{d}t = R_h^c - R_h^{gr} - R_h^r + \xi_h(t), \tag{11}$$

$$\dot{v} = \mathrm{d}v/\mathrm{d}t = R_v^c - R_v^e - R_i^c + \xi_v(t). \tag{12}$$

Here, the time-averaged (non-fluctuating) rates can be computed from the rate equations (1)–(9): R_h^c = rate of helium capture, R_h^{gr} = rate of helium replacement, R_h^r = rate of helium re-solution, R_v^e = rate of vacancy emission, and R_i^c = rate of interstitial capture. Stochastic fluctuations are represented by the random "forces" $\xi_h(t)$ and $\xi_v(t)$. These random components have a zero time-average, but are characterized by an amplitude and a spectrum. Cascade-induced fluctuations in point-defect concentrations have been studied by Mansur et al. [16], Marwick [17], and Chou and Ghoniem [18]. Fig. 2 shows the relative value of the root-mean-square (RMS) fluctuation in vacancy concentrations as a function of the cascade radius [18]. It is to be noted that the amplitude of the fluctuation is quite significant, and this will be reflected in the random function, $\xi_v(t)$. It is interesting to see that as the cascade size increases, the fluctuation amplitude decreases for cascades with a radius greater than ~ 400 Å. Cascades initiated by 14 MeV neutrons can be several thousand angstroms in size and may, therefore, result in a lower fluctuation amplitude, as compared with fission neutrons. Since the frequency range of the fluctuation spectrum is much higher than inverse relaxation times in cluster phase space, the average value of the phase-space vector can be described by trajectories, each being determined by the initial conditions. Those trajectories are solutions of eqs. (11) and (12), with the fluctuating functions $\xi_h(t)$ and $\xi_v(t)$ set to their time-averaged value of zero.

Stability of the HV cluster can be investigated by examining the phase-plane representation of the nodal lines given by $\mathrm{d}h/\mathrm{d}t = \mathrm{d}v/\mathrm{d}t = 0$. The critical points of the solution are obtained by the intersection of the line $\mathrm{d}h/\mathrm{d}t = 0$ with the line $\mathrm{d}v/\mathrm{d}t = 0$.

Numerical solutions of eqs. (11) and (12) have been implemented for the conditions of stainless steel irradiated in EBR-II (appm He/dpa = 0.1) and HFIR (appm He/dpa = 57). The results are shown in fig.

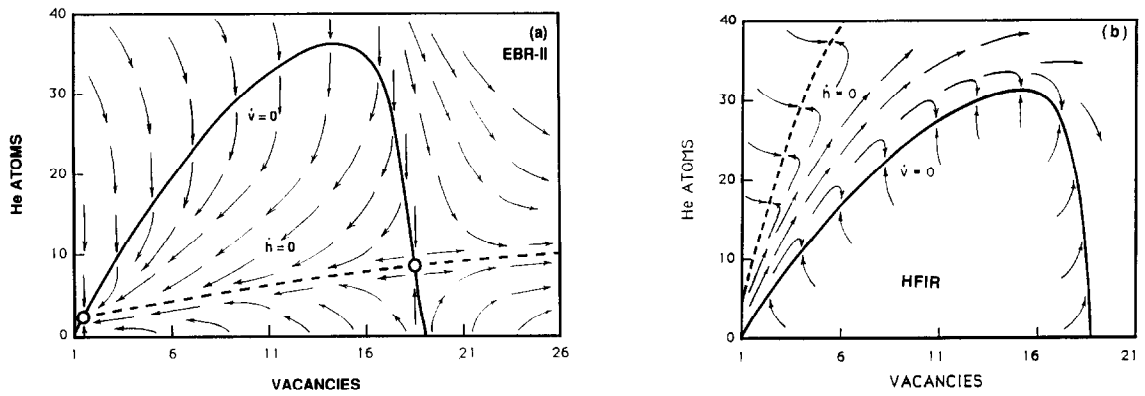

Fig. 3. Phase space representation of the flow field for (a) EBR-II and (b) HFIR conditions. Computations were made for a total sink density of $10^{10}\,\mathrm{cm}^{-2}$ and at 500 °C.

3, where the flow field in the HV phase space is represented by arrows. Fig. 3a illustrates that stochastic fluctuations (e.g., by cascades) are necessary to drive nucleation past the second critical point. On the other hand, it is shown that under high He-to-dpa conditions (fig. 3b), there are no critical points and the flow field propagates smoothly from any small cluster size (e.g., two helium atoms and a few vacancies) to larger ones. Nucleation is expected, therefore, to proceed without the need for stochastic fluctuations.

This phase-space analysis is useful in damage correlation studies. It can be used to determine if a given damage simulation experiment will lead to the same nucleation and cluster stability conditions as in a fusion reactor.

If the critical HV-cluster size is assumed to contain three helium atoms and one vacancy (see fig. 3b), the nucleation rate can be calculated from the forward reaction rates of eq. (7):

$$\frac{\mathrm{d}C_{\mathrm{tot}}}{\mathrm{d}t} = |\boldsymbol{J}|^* = 3(\beta C_{\mathrm{g}} + \gamma C_{\mathrm{v}})C^*. \tag{13}$$

The critical nucleus concentration is denoted by C^*. In eq. (13), it is assumed that nucleation is driven by further absorption of helium atoms and vacancies at existing clusters which contain three helium atoms. This is a simplified form of the nucleation current, but this simplification is possible because of the high He-to-dpa ratio.

In the present development, the nucleation current $\boldsymbol{J}^*$ has two components which represent one of the boundary conditions to the flow field (shown in fig. 3). The helium- and vacancy-driven components can be represented by, respectively, J_{h} and J_{v}. Thus

$$\boldsymbol{J}^* = J_{\mathrm{h}}\boldsymbol{i} + J_{\mathrm{v}}\boldsymbol{j}, \tag{14}$$

where $\boldsymbol{i}$ and $\boldsymbol{j}$ are unit vectors in the helium and vacancy directions, respectively.

Fig. 4 shows results of calculation for the total density of HV clusters for the conditions of dual ion-beam irradiation of steel at 625 °C [19]. The He-to-dpa ratio is 5 appm He/dpa and the displacement damage rate is 3×10^{-3} dpa/s. Continuous nucleation is clearly evident in the experimental results. Our study of the re-solution parameter, b' (the probability of gas re-solution into the matrix per dpa) shows that an average value of b on the order of unity is consistent with these experiments. The exact value of b should be determined from theoretical comparisons with experiments under the specific damage conditions. This value represents an average over the cavity size distribution and is quite important in explaining the continuous nucleation of cavities.

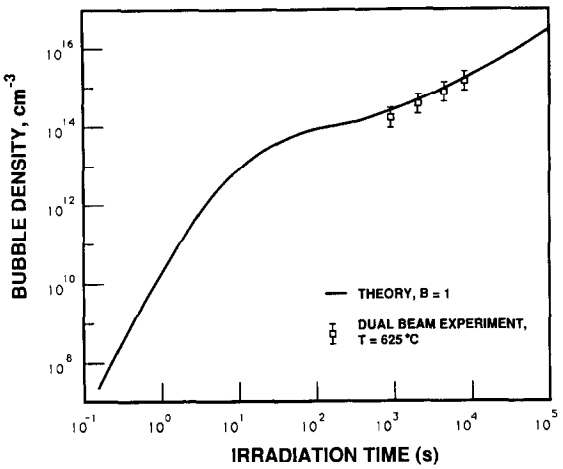

Fig. 4. Comparison between calculations and experiments for HV-cluster density of steel irradiated at 625 °C and 3×10^{-3} dpa/s.

4. The Fokker–Planck description of cavity evolution

The concentration of clusters containing h helium atoms and v vacancies at time t is given by

$$C(h, v, t)\,\mathrm{d}h\,\mathrm{d}v = C_{\mathrm{tot}}(t)P(h, v, t)\,\mathrm{d}h\,\mathrm{d}v, \tag{15}$$

where $P(h, v, t)\,\mathrm{d}h\,\mathrm{d}v$ is the probability of finding a cluster in the size interval $(h, v \to H + \mathrm{d}h, v + \mathrm{d}v)$. The time evolution of the probability function in terms of all possible transitions in the HV phase space is given by the master equation

$$\frac{\mathrm{d}P(h, v, t)}{\mathrm{d}t} = \sum_k W\{[(h-\Delta h_k), (v-\Delta v_k)] \to (h, v)\}P[(h-\Delta h_k), (v-\Delta v_k), t] - \sum_k W\{(h, v) \to [(h+\Delta h_k), (v+\Delta v_k)]\}P(h, v, t). \tag{16}$$

Here Δh_k and Δv_k are fluctuations in the helium and vacancy contents, respectively, which are caused by a stochastic process, k. We have shown that when the transition probability, W, and the cluster probability density, P, are both expanded around the point (h, v), one obtains the 2D Fokker–Planck equation given by

$$\frac{\partial P}{\partial t} + \nabla \cdot \boldsymbol{J} = 0, \tag{17}$$

where

$$\boldsymbol{J} = \boldsymbol{F}P - \nabla(\boldsymbol{D}P), \tag{18}$$

$$\boldsymbol{F} = \begin{bmatrix} a_{1\mathrm{h}} \\ a_{1\mathrm{v}} \end{bmatrix} \tag{19}$$

is a drift vector and

$$\boldsymbol{D} = \begin{bmatrix} a_{2\mathrm{hv}} & a_{2\mathrm{hh}} \\ a_{2\mathrm{vv}} & a_{2\mathrm{vh}} \end{bmatrix} \tag{20}$$

is a diffusion tensor. The components in eqs. (19) and (20) represent first and second moments of the transition probability. Details of the derivation of eqs. (17)–(20) can be found in ref. [20]. It is noted, however, that while cascade-induced fluctuations do not affect the magnitude of the first moments ($a_{1\mathrm{h}}$

and a_{1v}), they increase the magnitudes of the second moments (a_{2hh} and a_{2hv}). This can be seen by referring back to fig. 3.

Numerical solution of eq. (17) on an infinite quarter phase plane is given in ref. [20]. In this paper, a two-moment solution is presented for simplicity. Under these conditions, the rates of helium (k^{gc}), vacancy (k^{vc}) and interstitial (k^{ic}) capture, helium replacement (k^{gr}), and vacancy emission (k^{ve}) can be used to compute the elements of $\boldsymbol{F}$ and $\boldsymbol{D}$. These are given by

$$a_{1h} = k^{gc} - (k^{ge} + k^{gr}), \tag{21}$$

$$a_{1v} = k^{vc} - (k^{ic+ve} + k^{gr}), \tag{22}$$

$$a_{2hh} = \tfrac{1}{2}[k^{ge} + k^{gr} + k^{gc}], \tag{23}$$

$$a_{2vv} = \tfrac{1}{2}[k^{ic+ve} + k^{gr} + k^{vc}], \tag{24}$$

$$a_{2hv} = a_{2vh} = k^{gr}. \tag{25}$$

5. Approximate two-moment solution of the Fokker–Planck equation

The Fokker–Planck equation (eq. (17)) must be solved for the evolution of the probability density, P, in order to determine the nature of the evolving HV clusters. A numerical solution, which is coupled with the transient nucleation conditions (eq. (13)), has been developed by Sharafat and Ghoniem [20] for eq. (17). Denoting the cluster size by the vector $\boldsymbol{x}$, such that

$$\boldsymbol{x} = h\boldsymbol{i} + v\boldsymbol{j}, \tag{26}$$

and taking the first moment of eq. (17), we obtain

$$\mathrm{d}\langle \boldsymbol{x}\rangle/\mathrm{d}t = \langle \boldsymbol{F}(\boldsymbol{x})\rangle, \tag{27}$$

where the right-hand side represents the drift vector averaged over the probability distribution function. The symbol $\langle\ \rangle$ is used to denote this average. Eq. (27) is not a closed equation because of the nonlinearlity of $\boldsymbol{F}$. However, to lowest order, one can approximate this equation by

$$\mathrm{d}\langle \boldsymbol{x}\rangle/\mathrm{d}t = \boldsymbol{F}(\langle \boldsymbol{x}\rangle). \tag{28}$$

The integration of eq. (28) gives the trajectory of the average cluster in the growth regime of the flow field shown in fig. 3.

Let us define the variance matrix by

$$\langle \delta X_i \delta X_j\rangle = \langle X_i X_j\rangle - \langle X_i\rangle\langle X_j\rangle \quad i,j = \mathrm{h,v}. \tag{29}$$

Kinetic equations for the variance matrix can be shown to be given by [17]:

$$\frac{\mathrm{d}}{\mathrm{d}t}\langle \delta X_i \delta X_j\rangle = \langle X_i a_{ij}\rangle - \langle X_i\rangle\langle a_{ij}\rangle + \langle X_j a_{1i}\rangle - \langle X_j\rangle\langle a_{1i}\rangle + \langle a_{2,ij}\rangle. \tag{30}$$

Eq. (30) is again not closed, and expansions of the parameters around their values at the average trajectory, $\langle \boldsymbol{x}\rangle$, would result in an open-ended set of moment equations. Although it is possible to develop coupled equations for higher order moments (see ref. [22]), it is sufficient here to develop a lowest order expansion of eq. (30):

$$\frac{\mathrm{d}}{\mathrm{d}t}\langle \delta X_i \delta X_j\rangle \simeq a_{2,ij}(\langle \boldsymbol{x}\rangle). \tag{31}$$

Eq. (31) is the lowest order evolution equation for the variance matrix. The second moments of the transition probabilities, $a_{2,ij}$, are the components of the diffusion tensor (eq. (20)), and are to be evaluated at the average trajectory, $\boldsymbol{x}$.

We will proceed here by reconstructing the probability density function from its zeroth, first, and second moments. The simplest reconstruction procedure can be based on Gaussian functions, i.e.,

$$P(h, v, t) \simeq \left(\delta X_h \delta X_v \sqrt{2\pi}\right)^{-1} \exp(-y^2/2), \tag{32}$$

where

$$y = \left[\left(\frac{h - \langle h\rangle}{\delta X_h}\right)^2 + \left(\frac{v - \langle v\rangle}{\delta X_v}\right)^2\right]^{1/2}. \tag{33}$$

6. The effects of helium and collision cascades on cavity evolution

The formulation presented in the previous section permits study of the effects of simultaneous helium generation and cascade-induced point-defect fluctuations on cavity evolution. This is certainly useful for extrapolating existing radiation damage data to anticipated fusion conditions where the primary differences in damage parameters are the helium generation rate and the cascade size. Fig. 5 illustrates the propagation of the probability distribution function in size space under typical HFIR and EBR-II-type irradiation conditions for stainless steel at 500 °C. The He-to-dpa ratio plays an important role in determining the character of the distribution function. Both the HFIR and EBR-II reactors have similar displacement damage rates of $\sim 10^{-6}$ dpa/s, but differ in the He-to-dpa ratio (i.e., 57 for HFIR and 0.1 for EBR-II). The effects of this large difference between the ratios on the spread of the size distribution can be seen clearly in fig. 5. The low He-to-dpa ratio, characteristic of EBR-II, results in a smaller spread in helium content, and helium plays a small role in cavity evolution. (Notice the different scales between figs. 5a and 5b). In both cases, however, most of the cavities are not in thermodynamic equilibrium where the gas pressure is balanced by surface tension force [20].

Cascade effects on the cavity size distribution are included through the second moments of the transition probabilities in the Fokker–Planck equation. Cascades induce fluctuations in point-defect

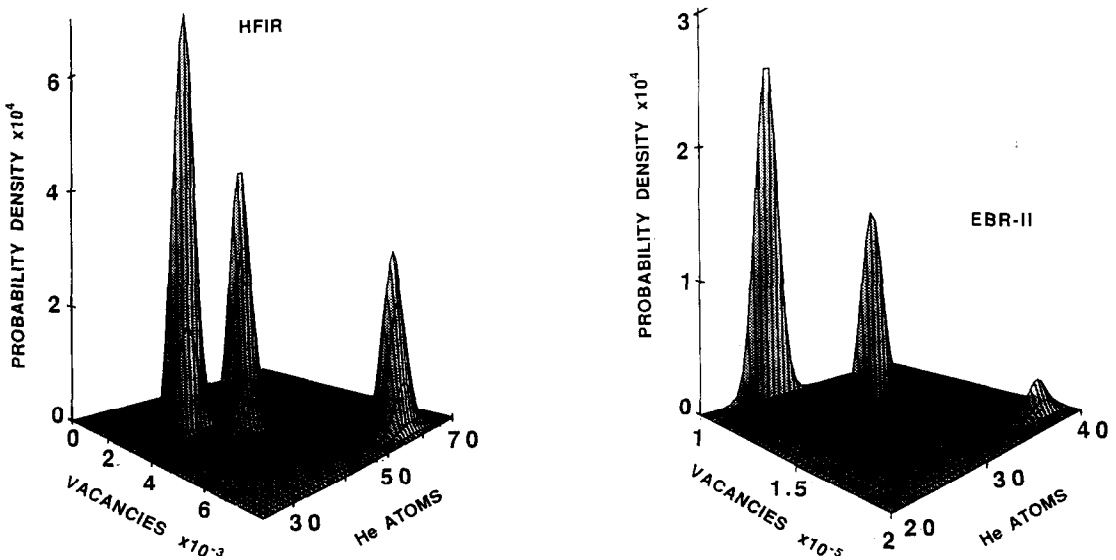

Fig. 5. Probability distribution function for HV clusters under irradiation of stainless steel at 500 °C for HFIR and EBR-II.

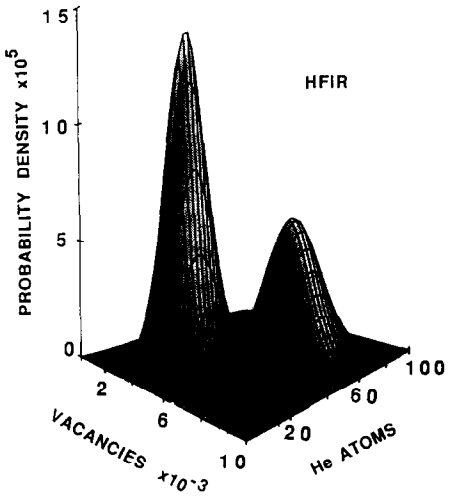

Fig. 6. The effects of a fourfold increase in the point-defect fluctuation amplitude on the probability distribution function for HV clusters under irradiation of stainless steel at 500 °C.

concentrations, as previously shown in fig. 2. Since the RMS value of the fluctuation depends on the cascade size, we must determine a spectrally averaged value for the variances δX_h and δX_v. We will treat this problem parametrically here, where we assume that cascades do not change the value of δX_h but simply increase δX_v. Fig. 6 shows the anticipated effects of cascades on the spread of the same size distribution as shown for HFIR conditions in fig. 5. Cascades were assumed to result in a fourfold increase in the magnitude of δX_v. The point to be made here is that a "broad" size distribution is indicative of an important effect of cascades. Without a systematic experimental/theoretical study, it is difficult to be more quantitative about the effects of cascades on cavity evolution.

7. Conclusions

Cavity evolution under conditions of cascade damage and high helium generation, which are typical of fusion reactor conditions, is shown to be a continuous process which cannot be easily separated into the classical nucleation and growth regimes. It is also emphasized that the rate of helium transport, which is described as an effective helium mobility, has a strong dependence on HV-cluster evolution. The long transient, associated with high helium mobility, is a result of the concentration build-up of small HV clusters which act as the primary traps for migrating helium. However, the quasi-steady-state mobility can be understood in terms of three simple mechanisms: radiation displacement at low temperatures, interstitial replacement at intermediate temperatures, and thermal desorption at high temperatures.

The displacement of helium by cascades from HV clusters results in significant effects on cavity evolution. First, this displacement process provides for an internal source of helium production which, in turn, causes continuous cavity nucleation. Second, the resulting fine distribution of helium nuclei in the matrix is associated with slower growth rates for helium-filled cavities.

The stochastic framework represented by Fokker–Planck theory is shown to be a convenient approach to the analysis of cavity evolution under fusion and simulation conditions. Although the major features of cavity evolution are included in this framework, its utility can be fully exploited by a systematic experimental approach where the basic parameters of the model can be clearly determined.

Nomenclature

f	Fraction of point defects surviving in-cascade recombination
G	Displacement damage rate
$C_s^{v,i}$	Equivalent matrix distributed point-defect sink density (i.e., for dislocations, cavities, and grain boundaries)
G_H	Helium generation rate
m	Average number of helium atoms in a cavity
C_{tot}	Total cavity density
M_{gb}	Helium concentration at grain boundaries
M_{ppt}	Helium concentration at precipitate interfaces
ϵ	Matrix cavity combinatorial number
ϵ_{ppt}	Precipitate cavity combinatorial number
C_{ppt}	Precipitate concentration
C_{gb}	Equivalent distributed sink for grain boundaries

Acknowledgements

This work was supported by the US Department of Energy, Office of Fusion Energy, Grant No. DE-FG03-84ER52110, with UCLA. The author wishes to acknowledge Drs. B. Singh, M. Victoria, and W.V. Green, for their efforts on behalf of the Workshop on Radiation Damage Correlation for Fusion Conditions.

References

[1] J.L. Katz and H. Wiedersich, J. Chem. Phys. 55 (1971) 1414.
[2] K.C. Russell, Acta Metall. 19 (1971) 753.
[3] G.W. Greenwood, J. Nucl. Mater. 4 (1959) 305.
[4] H. Trinkaus, J. Nucl. Mater. 118 (1983) 39.
[5] H. Trinkaus, Radiat. Eff. 101 (1986) 91.
[6] A.D. Brailsford and R. Bullough, J. Nucl. Mater. 48 (1973) 87.
[7] R. Bullough, B. Eyre and K. Krishan, Philos. Trans. R. Soc. London, Ser. A346 (1975) 81.
[8] W.F. Wolfer and M. Ashkin, J. Appl. Phys. 46 (1975) 547.
[9] L.K. Mansur, Nucl. Technol. 40 (1978) 5.
[10] N.M. Ghoniem and G.L. Kulcinski, Radiat. Eff. 39 (1978) 47.
[11] K. Krishan, Radiat. Eff. 66 (1982) 121.
[12] N.M. Ghoniem, J. Alhajji and D. Kaletta, J. Nucl. Mater. 136 (1985) 192.
[13] N.M. Ghoniem, S. Sharafat, J.M. Williams and L.K. Mansur, J. Nucl. Mater. 117 (1983) 96.
[14] A. Forman and B. Singh, J. Nucl. Mater. 141–143 (1986) 672.
[15] K.C. Russell, Acta Metall. 26 (1978) 1615.
[16] L.K. Mansur, W.A. Coghlan and A.D. Brailsford, J. Nucl. Mater. 85 & 86 (1979) 591.
[17] A.D. Marwick, J. Nucl. Mater. 116 (1983) 40.
[18] P. Chou and N.M. Ghoniem, J. Nucl. Mater. 137 (1985) 63.
[19] G. Ayrault, H.A. Hoff, F.V. Nolfi, Jr. and A.P.L. Turner, J. Nucl. Mater. 103 & 104 (1981) 1035.
[20] S. Sharafat and N.M. Ghoniem, Radiat. Eff. and Def. in Solids 113 (1990) 331.
[21] G. Nicolis and I. Prigogine, Self-Organization in Non-Equilibrium Systems (Wiley, New York, 1977) p. 254.
[22] N.M. Ghoniem, Phys. Rev. B39 (1989) 11810.